JOURNAL OF COMPUTATIONAL PHYSICS 8, 313–342 (1971)

An Implicit Monte Carlo Scheme for Calculating Time and Frequency Dependent Nonlinear Radiation Transport*

J. A. FLECK, JR. AND J. D. CUMMINGS

Lawrence Radiation Laboratory, University of California, Livermore

Received January 13, 1971

A flexible and accurate method for solving nonlinear, frequency-dependent radiative transfer problems by a Monte Carlo technique is developed. The method is based upon the concept of effective scattering, wherein a fraction of the radiative energy absorbed is instantaneously and isotropically reradiated in a manner analogous to a scattering process. The method appears to be unconditionally stable, conserves energy exactly, and is suitable for handling either transparent or optically thick media.

INTRODUCTION

Several authors have experimented with Monte Carlo methods for solving time-dependent nonlinear radiation transport problems [1, 2]. Unfortunately, certain deficiencies in the method as hitherto formulated have restricted both its flexibility and range of applicability. For optically thin systems in which the radiation field is well out of equilibrium with the matter, the method has been reasonably successful, but for systems with even moderately large absorption cross-sections, and for systems, generally, which are close to thermodynamic equilibrium the method has exhibited objectionable features which include unacceptably large fluctuations, large energy imbalances, and the requirement of unreasonably small integration cycle times. We wish in this article to describe a wholly new approach to the Monte Carlo solution of nonlinear radiation problems, which in some measure appears to remove all of the objectionable features mentioned above, and which provides an accurate and highly flexible calculational tool applicable to a wide variety of frequency-dependent problems. The "implicitness" of the method is to be interpreted in the sense that the radiation field and the material energy density are calculated in a self-consistent manner analogous to the implicit finite difference solution of coupled matter and radiation equations describing nonequilibrium frequency-dependent radiation diffusion theory [3, 4].

* This work was performed under the auspices of the U. S. Atomic Energy Commission.

581/8/3-1

As in the case of the finite difference solution, the implicitness of the Monte Carlo calculation apparently leads to unconditional stability [5].

The basis of all Monte Carlo solutions of radiative transfer problems is the generation of radiation energy bundles or "particles" [6] from sources which have been calculated on the basis of a current knowledge of the temperature distribution. A novel feature of the present Monte Carlo scheme is that only a fraction of the total source energy is actually treated in this manner. The remaining fraction is treated as though it resulted from an isotropic scattering process. The resulting radiation transport equation contains, in addition to the normal scattering terms, "effective" scattering terms which may be interpreted physically as the absorption and isotropic reemission of radiation [7]. Correspondingly, the true frequency-dependent absorption cross section can be regarded as composed in part of effective absorption and effective scattering. The portion of the true absorption cross section devoted to effective scattering depends on the integration cycle time, Planck mean cross section, and temperature.

The concept of effective scattering is an exceedingly useful one for several reasons. Without it the absorption of radiation particles and their redistribution in angle and frequency from newly created temperature dependent sources must be carried out over exceedingly short integration cycle times if the medium is strongly absorbing. If effective scattering is employed under these circumstances, arbitrary integration cycle times can be used, and the absorption and recreation of photons takes place as an instantaneous scattering process with an actual enhancement in the accuracy of the calculation. The enhancement in accuracy comes about because photons are reemitted from the place in which they were absorbed which is what occurs physically. In the more conventional Monte Carlo treatment, on the other hand, photons are absorbed but reemitted in a distribution which normally is uniform in position over the entire spatial cell in which the temperature is assumed constant, with a consequent loss in information. When effective scattering is used and the medium is strongly absorbing, the only important effect of spatially discretizing the temperature is on the variation of the cross sections. Otherwise the spatial and, for that matter, the temporal accuracy of the source term in the radiation transfer equation should be limited only by fluctuations inherent in the Monte Carlo process. The accuracy with which source terms are treated suggests that the resulting Monte Carlo solution to the nonlinear radiation transfer problem should be valid under circumstances when diffusion theory normally applies [8]. That the Monte Carlo treatment simulates a diffusion process in strongly absorbing situations in a natural way is evident from the fact that the effective scattering cross section becomes nearly equal to the true absorption cross section, and the transport of radiation is governed almost entirely by isotropic scattering with a short mean free path.

A frequent bugaboo of radiative transfer calculations is that a medium may

be transparent to certain frequencies but opaque to others. When effective scattering is employed, this situation offers no difficulty, since radiation is strongly scattered from the opaque regions of the spectrum to the transparent, where it is more easily transported. An additional advantage of employing effective scattering is that it enables the emission spectrum to be sampled in a much more complete way, since a sampling of the emission spectrum takes place with every scattering event. Otherwise an insufficient number of source particles might be available for sampling from a complicated spectrum. The end result of the effective scattering treatment of absorption and emission is a highly flexible and foolproof method of calculation.

The outline of the paper is briefly as follows. In Sections I–III the basic form of the radiative transfer equation is derived, including effective scattering terms. The resulting equation is perfectly general and may be solved by any feasible means, although the scattering aspects of the problem make the Monte Carlo method a particularly attractive candidate. Section IV is devoted to the details of a Monte Carlo solution of the problem, which turn out to be quite straightforward. Finally, a variety of numerical illustrations is provided in Section IV.

I. Single Frequency or Grey Approximation

For simplicity, we begin our discussion by considering the grey case without scattering in one-dimensional slab geometry. The equations are, assuming local thermodynamic equilibrium,

$$\frac{1}{c}\frac{\partial I}{\partial t} + \mu\frac{\partial I}{\partial x} + \sigma I = \frac{1}{2}\sigma acT^4, \tag{1.1a}$$

$$\frac{\partial u_m}{\partial t} = \sigma\left(\int_{-1}^{1} I\,d\mu - acT^4\right) + S. \tag{1.1b}$$

Here $I(x, t, \mu)$ is the specific intensity, T is the material temperature, u_m is the material energy density, μ is the x-component of the direction vector, a is the radiation energy density constant, and S is an arbitrary source function. The addition to Eq. (1.1a) of terms representing Thomson scattering leads to no complications and will not be considered here. It is convenient to introduce the equilibrium radiation energy density variable

$$u_r = aT^4 \tag{1.2}$$

instead of T.

Defining

$$\frac{\partial u_m}{\partial u_r} = \beta^{-1}, \tag{1.3}$$

we may write Eqs. (1.1) as

$$\frac{1}{c}\frac{\partial I}{\partial t} + \mu\frac{\partial I}{\partial x} + \sigma I = \frac{1}{2}c\sigma u_r, \tag{1.4a}$$

$$\frac{\partial u_r}{\partial t} = \beta\sigma\left(\int_{-1}^{1} I\,d\mu - cu_r\right) + \beta S. \tag{1.4b}$$

By means of Eqs. (1.2) and (1.3) the problem's nonlinearity can be characterized by a single multiplicative factor β in Eq. (1.4b). The usefulness of this form of the matter energy balance equation for Monte Carlo application will become apparent. In the case of a perfect gas with constant specific heat one can take

$$u_m = bT, \tag{1.5}$$

where b is independent of temperature. The factor β then becomes

$$\beta = \frac{\partial u_r}{\partial u_m} = \frac{4aT^3}{b} = \frac{4u_r}{u_m}. \tag{1.6}$$

If Eq. (1.4b) is integrated over an integration cycle from time t^n to t^{n+1}, the result is

$$u_r^{n+1} - u_r^n = \int_{t^n}^{t^{n+1}} dt\,\beta\sigma\int_{-1}^{1} I\,d\mu - c\int_{t^n}^{t^{n+1}} dt\,\beta\sigma u_r + \int_{t^n}^{t^{n+1}} dt\,\beta S, \tag{1.7a}$$

where $u_r^n = u_r(x, t^n)$. If appropriate average values of the integrands are factored outside the integrals over time, Eq. (1.7a) becomes

$$u_r^{n+1} - u_r^n = \Delta t\bar{\beta}\bar{\sigma}\left\{\int I^\lambda\,d\mu - c[\alpha u_r^{n+1} + (1-\alpha)u_r^n]\right\} + \bar{\beta}S^\gamma\Delta t. \tag{1.7b}$$

Here $\Delta t = t^{n+1} - t^n$, and the superscripts λ, γ, and the coefficient α define the time centering, as yet unspecified, of the mean values of I, S, and u_r. Solving (1.7b) for u_r^{n+1}, yields

$$u_r^{n+1} = \left[\frac{1-(1-\alpha)\beta c\,\Delta t\sigma}{1+\alpha\beta c\,\Delta t\sigma}\right]u_r^n + \frac{\beta\sigma\,\Delta t}{1+\alpha\beta c\,\Delta t\sigma}\int I^\lambda\,d\mu + \frac{\beta\Delta t S^\gamma}{1+\alpha\beta c\,\Delta t\sigma}, \tag{1.8}$$

where, for simplicity, bars over β and σ have been omitted. We are interested in an appropriately centered value of u_r, which we write as

$$\begin{aligned} u_r^\gamma &= \alpha u_r^{n+1} + (1-\alpha)u_r^n \\ &= \frac{\alpha\beta\sigma\,\Delta t}{1+\alpha\beta c\,\Delta t\sigma}\int I^\lambda\,d\mu + \frac{u_r^n}{1+\alpha\beta c\,\Delta t\sigma} + \frac{\alpha\beta\,\Delta t S^\gamma}{1+\alpha\beta c\,\Delta t\sigma}. \end{aligned} \tag{1.9}$$

We now rewrite the transport Eq. (1.4a) with u_r^{γ} substituted for u_r to obtain

$$\frac{1}{c}\frac{\partial I}{\partial t} + \mu\frac{\partial I}{\partial x} + \sigma I = \frac{1}{2}c\sigma u_r^{\gamma} = \frac{1}{2}\sigma\left(\frac{\alpha\beta c\,\Delta t\sigma}{1+\alpha\beta c\,\Delta t\sigma}\right)\int I^{\lambda}\,d\mu + \frac{1}{2}\left(\frac{c\sigma u_r^{n}}{1+\alpha\beta c\,\Delta t\sigma} + \frac{\sigma\alpha\beta c\,\Delta t S^{\gamma}}{1+\alpha\beta c\,\Delta t\sigma}\right), \tag{1.10}$$

which is presumed to be accurate over a time Δt. If, however, we substitute the instantaneous value of I for I^{λ}, Eq. (1.10) becomes the following transport equation for an isotropic scattering problem with a time-independent source function.

$$\frac{1}{c}\frac{\partial I}{\partial t} + \mu\frac{\partial I}{\partial x} + \sigma I = \frac{1}{2}\sigma\left(\frac{\alpha\beta c\,\Delta t\sigma}{1+\alpha\beta c\,\Delta t\sigma}\right)\int I\,d\mu + \frac{1}{2}\left(\frac{c\sigma u_r^{n}}{1+\alpha\beta c\,\Delta t\sigma} + \frac{\sigma\alpha\beta c\,\Delta t S^{\gamma}}{1+\alpha\beta c\,\Delta t\sigma}\right). \tag{1.10a}$$

Here the total cross section σ can be thought of as being made up of effective absorption and scattering contributions σ_a and σ_s, where

$$\sigma_a = \frac{1}{1+\alpha\beta c\,\Delta t\sigma}\sigma, \tag{1.11a}$$

$$\sigma_s = \frac{\alpha\beta c\,\Delta t\sigma}{1+\alpha\beta c\,\Delta t\sigma}\sigma, \tag{1.11b}$$

Obviously, as Δt becomes larger the effective scattering contribution becomes larger. In fact, as $\Delta t \to \infty$, Eq. (1.10a) becomes

$$\frac{1}{c}\frac{\partial I}{\partial t} + \mu\frac{\partial I}{\partial x} + \sigma I = \frac{1}{2}\sigma\int I\,d\mu + \frac{1}{2}\sigma S^{\gamma} \tag{1.12}$$

which always has a well-behaved Monte Carlo solution. The steady state solution of Eq. (1.12) in the absence of a source term satisfies the well-known form of the equation of transfer

$$\mu\frac{\partial I}{\partial x} + \sigma I = \frac{1}{2}\sigma\int I\,d\mu, \tag{1.13}$$

which describes the transport of radiation under conditions of radiative equilibrium [9].

It should be remarked that if one differences Eq. (1.10a) in time, replacing I with I^{λ} in all nonderivative terms, one obtains exactly the same equation which one would have obtained had one proceeded by differencing Eqs. (1.1a) and (1.1b) in time from the start. This assures us that the Monte Carlo solution to Eq. (1.10a) will correspond to the solution of the appropriately time centered difference versions of Eqs. (1.1a) and (1.1b).

In order to further test the consistency of the transport equation in the form (1.10a) with Eqs. (1.7) describing the material energy balance, we integrate (1.10a) over direction to obtain

$$\frac{1}{c}\frac{\partial}{\partial t}\int I\,d\mu + \frac{\partial F}{\partial x} = -\sigma\int I\,d\mu + \sigma\left(\frac{\alpha\beta c\,\Delta t\sigma}{1+\alpha\beta c\,\Delta t\sigma}\right)\int I\,d\mu + \frac{\alpha\beta c\,\Delta t\sigma S^{\nu}}{1+\alpha\beta c\,\Delta t\sigma} + \frac{c\sigma}{1+\alpha\beta c\,\Delta t\sigma}u_r^{\,n}$$

$$= -\frac{1}{\beta}\frac{\partial u_r}{\partial t} + S^{\nu} \tag{1.14}$$

where the radiation flux F is defined by

$$F = \int \mu I\,d\mu. \tag{1.15}$$

The second equality in (1.14) is simply a statement of energy conservation, implying that the net loss rate for radiation energy density must contribute an equivalent rate of gain of the material energy density. If we integrate Eq. (1.14) over the cycle time Δt, we obtain

$$u_r^{n+1} = u_r^{\,n} + \frac{\beta\sigma}{1+\alpha\beta c\,\Delta t\sigma}\int_{t^n}^{t^{n+1}} dt\int I\,d\mu - \frac{\alpha\beta c\,\Delta t\sigma}{1+\alpha\beta c\,\Delta t\sigma}u_r^{\,n} + \frac{\beta\Delta t S^{\nu}}{1+\alpha\beta c\,\Delta t\sigma}. \tag{1.15a}$$

Combining the coefficients of $u_r^{\,n}$, one gets

$$u_r^{n+1} = \frac{\beta\sigma}{1+\alpha\beta c\,\Delta t\sigma}\int_{t^n}^{t^{n+1}} dt\int I\,d\mu + \frac{1-(1-\alpha)\beta c\,\Delta t\sigma}{1+\alpha\beta c\,\Delta t\sigma}u_r^{\,n} + \frac{\beta\Delta t S^{\nu}}{1+\alpha\beta c\,\Delta t\sigma}. \tag{1.15b}$$

It is seen that Eqs. (1.15b) and (1.8) become identical provided that we make the identification

$$\int_{t^n}^{t^{n+1}} dt\int I\,d\mu \to \Delta t\int I^{\nu}\,d\mu, \tag{1.16}$$

which was previously assumed in deriving Eq. (1.7b) from Eq. (1.7a). Thus, we can be sure that a numerical solution of Eq. (1.10a) followed by a solution of Eq. (1.15b) will lead to self-consistent numerical solutions, satisfying the basic equations (1.4a) and (1.4b). However, a scheme for updating the material energy density which is much superior in practice is obtained as follows. Equation (1.14) may, after collection of the integral terms, be written as

$$\frac{\partial u_m}{\partial t} = \frac{\sigma}{1+\alpha\beta\sigma c\,\Delta t}\int I\,d\mu - \frac{c\sigma u_r^{\,n}}{1+\alpha\beta c\,\Delta t\sigma} + \frac{S^{\nu}}{1+\alpha\beta c\,\Delta t\sigma}. \tag{1.17}$$

The first term on the right side of Eq. (1.17) represents the rate of material heating due to effective absorptions. The second and third right terms represent effective emission and source heating rates. Obviously as the product $\alpha\beta c\Delta t\sigma$ goes to 0, Eq. (1.17) reduces to the material energy balance equation (1.1b) with u_r^n replacing u_r and S^ν replacing S. If Eq. (1.17) is integrated between t^n and t^{n+1}, the result is

$$u_m^{n+1} = u_m^n + \frac{\sigma}{1 + \alpha\beta c\,\Delta t\sigma}\int_{t^n}^{t^{n+1}} dt \int I\,d\mu - \frac{c\Delta t\sigma u_r^n}{1 + \alpha\beta c\,\Delta t\sigma} + \frac{S^\nu\,\Delta t}{1 + \alpha\beta c\,\Delta t\sigma}, \tag{1.18}$$

and assuming that u_m can be expressed by means of Eq. (1.5), we have

$$T^{n+1} = T^n + b^{-1}\left\{\frac{\sigma}{1 + \alpha\beta c\,\Delta t\sigma}\int_{t^n}^{t^{n+1}} dt \int I\,d\mu - \frac{c\Delta t\sigma u_r^n}{1 + \alpha\beta c\,\Delta t\sigma} + \frac{S^\nu\,\Delta t}{1 + \alpha\beta c\,\Delta t\sigma}\right\}. \tag{1.19}$$

For a nonperfect gas one substitutes $\partial u_m/\partial T$ for b in the above equation [10].

Equation (1.10a) may be solved by any method which is feasible, but because of the importance which scattering plays in the problem a Monte Carlo method of solution seems the most practical. Once the radiation field has been advanced and the absoprtion rate has been calculated, the temperature can be advanced using Eq. (1.19), which insures total energy conservation. The values of σ and β to be employed in the calculation are to be obtained either from temperatures available at t^n or by suitable forward extrapolation. Note that although σ or β may be reasonably rapidly varying functions of temperature, the product $\beta\sigma$ is normally much less rapidly varying due to the inverse dependence of σ on temperature. The centering parameter α should in general vary between $\frac{1}{2}$ and 1. For sufficiently small Δt it may be set equal to $\frac{1}{2}$, but for large values of $\alpha\beta c\Delta t\sigma$, α must be set equal to 1 or else the coefficient of u_r^n in Eq. (1.15b) will be negative, tending to cause oscillations in the solution of u_r from cycle to cycle.

It will be noted that one very fortunate aspect of the present calculational method is that even though the final solution is implicit in the sense defined in the introduction, in practice it involves entirely separate and independent transport and energy balance calculations.

II. Summary of Monte Carlo Procedure for Grey Case

The grey case Monte Carlo procedure can be briefly summarized as follows. Let us assume that I, T, and consequently u_r are known at time $t = t^n$, and that we wish to determine I, T, and u_r at time $t = t^{n+1} = t^n + \Delta t$. The initial conditions on the radiation field at time $t = t^n$ are provided by the census or "in transit" particles, and the temperature is assumed to be constant over each of a set of discrete zones of length Δx_j, $j = 1, 2, 3, \ldots, J$ [11].

1. From temperatures available at $t = t^n$, or by forward extrapolation, values of β and σ are determined for each spatial zone.

2. From S appropriately time-centered and u_r^n one calculates the sources appropriate to each space zone, generates new particles from the sources, and advances the solution to the transport equation

$$\frac{1}{c}\frac{\partial I}{\partial t} + \mu\frac{\partial I}{\partial x} + (\sigma_a + \sigma_s) I = \frac{1}{2}\sigma_s \int I\, d\mu + \frac{1}{2}\frac{c\sigma u_r^n}{1 + \alpha\beta c\, \Delta t\sigma} + \frac{1}{2}\frac{\sigma\alpha\beta c\, \Delta t S^\nu}{1 + \alpha\beta c\, \Delta t\sigma} \tag{2.1}$$

by standard Monte Carlo procedures, utilizing both the "old" census particles and the "new" source particles. The solution of Eq. (2.1) will consist of the information contained by the census particles at time $t = t^{n+1}$. Note that the nonscattering source terms in Eq. (2.1) are to be considered constant throughout the time cycle, which means that source particles will be emitted randomly in time over the time Δt.

3. In the process of advancing particles in the solution of Eq. (2.1) the quantities

$$\frac{\sigma}{1 + \alpha\beta c\, \Delta t\sigma}\int_{t^n}^{t^{n+1}} dt \int I\, d\mu \tag{2.2}$$

are determined by accumulating the particle energy deposited as the result of effective absorptions within each zone. The temperature solution is advanced by solving for each spatial zone, by iteration, the equation

$$T^{n+1} = T^n + b^{-1}(T)\left\{\frac{\sigma}{1 + \alpha\beta c\, \Delta t\sigma}\int_{t^n}^{t^{n+1}} dt \int I\, d\mu - \frac{c\Delta t\sigma u_r^n}{1 + \alpha\beta c\, \Delta t\sigma} + \frac{S^\nu\, \Delta t}{1 + \alpha\beta c\, \Delta t\sigma}\right\} \tag{2.3}$$

where $b(T)$ is given by

$$b(T) = \frac{\partial u_m}{\partial T} \tag{2.4}$$

for an appropriately time-centered value of T.

III. Frequency Dependent Case

In the frequency-dependent case without scattering we must solve instead of Eqs. (1.4) the equations

$$\frac{1}{c}\frac{\partial I_\nu}{\partial t} + \mu\frac{\partial I_\nu}{\partial x} + \sigma_\nu I_\nu = \frac{1}{2} c\sigma_\nu B_\nu\,, \tag{3.1a}$$

$$\frac{\partial u_r}{\partial t} = \beta\left\{\int\int \sigma_\nu I_\nu\, d\nu\, d\mu - c\int \sigma_\nu B_\nu\, d\nu\right\} + \beta S, \tag{3.1b}$$

where I_ν is a frequency-dependent specific intensity, and B_ν is the Planck or black-body distribution function.

Let us write

$$B_\nu = b_\nu u_r \,, \tag{3.2}$$

where b_ν is a normalized Planck spectrum at some time between t^n and t^{n+1}, to be obtained by forward extrapolation of temperature if necessary. Equations (3.1) become

$$\frac{1}{c}\frac{\partial I_\nu}{\partial t} + \mu\frac{\partial I_\nu}{\partial x} + \sigma_\nu I_\nu = \frac{1}{2}c\sigma_\nu b_\nu u_r \,, \tag{3.3a}$$

$$\frac{\partial u_r}{\partial t} = \beta\left(\int\int \sigma_\nu I_\nu \, d\nu \, d\mu - c\sigma_p u_r\right) + \beta S, \tag{3.3b}$$

where σ_p is the Planck mean absorption cross section defined by

$$\sigma_p = \int b_\nu \sigma_\nu \, d\nu.$$

By integrating Eq. (3.3b) from t^n to t^{n+1} we obtain the frequency-dependent analogs of Eqs. (1.7a) and (1.7b)

$$u_r^{n+1} - u_r^n = \int_{t^n}^{t^{n+1}} dt\,\beta\int\int \sigma_\nu I_\nu \, d\nu \, d\mu - c\int_{t^n}^{t^{n+1}} dt\,\beta\sigma_p u_r + \int_{t^n}^{t^{n+1}} dt\,\beta S, \tag{3.4a}$$

$$u_r^{n+1} - u_r^n = \bar{\beta}\,\Delta t\left\{\int\int \bar{\sigma}_\nu I_\nu^\lambda \, d\nu \, d\mu - c\bar{\sigma}_p[\alpha u_r^{n+1} + (1-\alpha)u_r^n]\right\} + \bar{\beta}S^\nu\Delta t. \tag{3.4b}$$

Solving for $u_r^\nu = \alpha u_r^{n+1} + (1-\alpha)u_r^n$, inserting into (3.3a) in the manner of Eqs. (1.9) and (1.10), and changing I_ν^λ to its instantaneous value leads to the following result:

$$\frac{1}{c}\frac{\partial I_\nu}{\partial t} + \mu\frac{\partial I_\nu}{\partial x} + \sigma_\nu I_\nu = \frac{1}{2}\sigma_\nu b_\nu\left[\frac{\alpha\beta c\,\Delta t}{1+\alpha\beta c\,\Delta t\sigma_p}\right]\int\int \sigma_{\nu'} I_{\nu'}\, d\nu'\, d\mu'$$
$$+ \frac{1}{2}\frac{c\sigma_\nu b_\nu u_r^n}{1+\alpha\beta c\,\Delta t\sigma_p} + \frac{1}{2}\frac{\sigma_\nu b_\nu \alpha\beta c\,\Delta t S^\nu}{1+\alpha\beta c\,\Delta t\sigma_p}. \tag{3.5}$$

The first integral on the right side of Eq. (3.5) represents a scattering source for an effective differential scattering cross section

$$\frac{d^2\sigma}{d\mu d\nu}(\nu' \to \nu) = \frac{1}{2}\sigma_{\nu'}\left[\frac{\sigma_\nu b_\nu \alpha\beta c\,\Delta t}{1+\alpha\beta c\,\Delta t\sigma_p}\right]. \tag{3.6}$$

Note that for this type of scattering, photon frequencies change, but no energy is exchanged with the matter. The total effective scattering cross section is gotten by integrating Eq. (3.6) over μ and the final frequency ν. The result is (reversing the roles of ν and ν'):

$$\sigma_{\nu s} = \sigma_\nu \left[\frac{\sigma_p \alpha\beta c\, \Delta t}{1 + \alpha\beta c\, \Delta t \sigma_p}\right], \tag{3.7a}$$

and the corresponding absorption cross section is

$$\sigma_{\nu a} = \sigma_\nu \left[\frac{1}{1 + \alpha\beta c\, \Delta t \sigma_p}\right] \tag{3.7b}$$

where $\sigma_\nu = \sigma_{\nu a} + \sigma_{\nu s}$. Note that the fractions of σ_ν devoted to absorption and scattering are independent of frequency. Equations (3.7a) and (3.7b) should be compared to Eqs. (1.11a) and (1.11b) for the grey case. If Eq. (3.5) is integrated over ν and μ, the result is

$$\begin{aligned}\frac{1}{c}\frac{\partial}{\partial t}\int\int d\nu\, d\mu\, I_\nu + \frac{\partial F}{\partial t} &= -\int\int d\nu\, d\mu\, \sigma_\nu I_\nu + \left(\frac{\alpha\beta c\, \Delta t \sigma_p}{1 + \alpha\beta c\, \Delta t \sigma_p}\right)\int\int d\nu\, d\mu\, \sigma_\nu I_\nu \\ &\quad + \frac{c\sigma_p u_r^{\,n}}{1 - \alpha\beta c\, \Delta t \sigma_p} + \frac{\sigma_p \alpha\beta c\, \Delta t S^\nu}{1 + \alpha\beta c\, \Delta t \sigma_p} \\ &= -\frac{\partial u_m}{\partial t} + S^\nu,\end{aligned} \tag{3.8}$$

where the radiation flux F is now defined by

$$F = \int\int I_\nu \mu\, d\mu\, d\nu. \tag{3.8a}$$

Combining terms, we get

$$\frac{\partial u_m}{\partial t} = \frac{1}{1 + \alpha\beta c\, \Delta t \sigma_p}\int\int d\nu\, d\mu\, \sigma_\nu I_\nu - \frac{c\sigma_p u_r^{\,n}}{1 + \alpha\beta c\, \Delta t \sigma_p} + \frac{S^\nu}{1 + \alpha\beta c\, \Delta t \sigma_p}. \tag{3.9}$$

Equation (3.8) should be compared to Eq. (1.14) and Eq. (3.9) to Eq. (1.17). The solution to Eq. (3.8) analogous to Eq. (1.15b) is

$$\begin{aligned}u_r^{n+1} &= \frac{\beta}{1 + \alpha\beta c\, \Delta t \sigma_p}\int_{t^n}^{t^{n+1}} dt \int\int d\nu\, d\mu\, \sigma_\nu I_\nu \\ &\quad + \frac{1 - (1 - \alpha)\beta c\, \Delta t \sigma_p}{1 + \alpha\beta c\, \Delta t \sigma_p} u_r^{\,n} + \frac{\beta S^\nu\, \Delta t}{1 + \alpha\beta c\, \Delta t \sigma_p},\end{aligned} \tag{3.10a}$$

while the solution analogous to Eq. (1.19) is

$$T^{n+1} = T^n + \frac{b^{-1}}{1 + \alpha\beta c\,\Delta t\sigma_p}\left\{\int_{t^n}^{t^{n+1}} dt \iint dv\, d\mu\, \sigma_\nu I_\nu - c\,\Delta t\sigma_p u_r^n + S^\nu\,\Delta t\right\}. \tag{3.10b}$$

Again, as in the grey case, for stable solutions of Eq. (3.10a) we require that

$$(1 - \alpha)\,\beta c\Delta t\sigma_p \leqslant 1. \tag{3.12}$$

The consistency between Eqs. (3.4) and the source terms in Eq. (3.5) is readily demonstrated by means of Eq. (3.10a).

It is easily shown that Eq. (3.4) is satisfied by the correct equilibrium solution $I_\nu = \frac{1}{2}cB_\nu$ when

$$\frac{\partial I_\nu}{\partial t} = \frac{\partial I_\nu}{\partial x} = 0. \tag{3.13}$$

Equation (3.5) becomes, in the absence of an external source term,

$$\sigma_\nu I_\nu = \frac{1}{2}\,\sigma_\nu b_\nu\left[\frac{\alpha\beta c\,\Delta t}{1 + \alpha\beta c\,\Delta t\sigma_p}\right]\iint \sigma_{\nu'} I_{\nu'}\, dv'\, d\mu' + \frac{1}{2}\,\frac{c\sigma_\nu b_\nu u_r}{1 + \alpha\beta c\,\Delta t\sigma_p}, \tag{3.14}$$

where the superscript on u_r has been dropped. If we set $I_{\nu'} = \frac{1}{2}cb_{\nu'}u_r$ in the integral term on the right side of Eq. (3.14), the equation becomes

$$\begin{aligned}\sigma_\nu I_\nu &= \frac{1}{2}\,\sigma_\nu b_\nu\left[\frac{\alpha\beta c\,\Delta t}{1 + \alpha\beta\sigma_p c\,\Delta t}\right]\sigma_p c u_r + \frac{1}{2}\,\sigma_\nu b_\nu\,\frac{cu_r}{1 + \alpha\beta\sigma_p c\,\Delta t} \\ &= \tfrac{1}{2}\sigma_\nu c b_\nu u_r = \tfrac{1}{2}\sigma_\nu c B_\nu\,.\end{aligned} \tag{3.15}$$

If

$$\frac{\partial I_\nu}{\partial t} = S^\nu = 0,$$

but gradients are present, Eq. (3.5) becomes, in the limit $\Delta t \to \infty$,

$$\mu\,\frac{\partial I_\nu}{\partial x} + \sigma_\nu I_\nu = \frac{1}{2}\,\frac{\sigma_\nu b_\nu}{\sigma_p}\iint \sigma_{\nu'} I_{\nu'}\, dv'\, d\mu'. \tag{3.16}$$

The form of Eq. (3.16), which is the frequency-dependent analog of Eq. (1.13), should be obvious from Eqs. (3.3) upon setting

$$\frac{\partial u_r}{\partial t} = \frac{\partial I_\nu}{\partial t} = S = 0,$$

i.e., the case of radiative equilibrium. The difficulty of solving Eq. (3.16) lies in the fact that σ_ν and b_ν depend on temperature, which must satisfy the relation

$$aT^4 = \frac{1}{c\sigma_p(T)} \int\int \sigma_\nu I_\nu \, d\nu \, d\mu. \tag{3.17}$$

But by utilizing Eqs. (3.5) and (3.10b) in a time-dependent approach and allowing the numerical solutions for T and I_ν to approach a steady state, the simultaneous pair of Eqs. (3.16) and (3.17) is readily solved.

IV. Monte Carlo Procedure Applied to the Frequency Dependent Case

For clarity we repeat the basic equations which must be solved in the absence of real scattering. These are

$$\frac{1}{c}\frac{\partial I_\nu}{\partial t} + \mu \frac{\partial I_\nu}{\partial x} + (\sigma_{\nu a} + \sigma_{\nu s}) I_\nu = \frac{1}{2}(1-f)(\sigma_\nu b_\nu/\sigma_p) \int\int \sigma_{\nu'} I_{\nu'} \, d\nu' \, d\mu' + \tfrac{1}{2} f c \sigma_\nu b_\nu u_r^n + \tfrac{1}{2}(1-f)(\sigma_\nu b_\nu/\sigma_p) S^\nu, \tag{4.1a}$$

$$\sigma_{\nu a} = f\sigma_\nu, \tag{4.1b}$$

$$\sigma_{\nu s} = (1-f)\sigma_\nu, \tag{4.1c}$$

$$f = \frac{1}{1 + \alpha\beta c \, \Delta t \sigma_p}, \tag{4.1d}$$

$$T^{n+1} = T^n + b^{-1}(T) f \left\{ \int_{t^n}^{t^{n+1}} dt \int\int \sigma_\nu I_\nu \, d\nu \, d\mu - c\Delta t \sigma_p u_r^n + S^\nu \Delta t \right\}. \tag{4.1e}$$

Again, in Eq. (4.1e) T represents an appropriately time-centered temperature.

The basic steps and considerations involved in a Monte Carlo solution of Eqs. (4.1a)–(4.1e) are outlined as follows

A. *Cross Section Data*

If the transport medium is optically thick and σ_ν contains considerable detailed structure, it may be necessary to calculate σ_ν by a table lookup procedure. For optically thick media, the effective scattering cross section is in general large, which leads to many scattering events. Each scattering event requires a new calculation of σ_ν, making it necessary to calculate σ_ν quickly. The spectrum $\sigma_\nu b_\nu$ must also be available under the same conditions requiring the tabulation of the quantities

$$F(\nu_k) = \int_0^{\nu_k} \sigma_\nu b_\nu \, d\nu, \tag{4.2a}$$

and ν_j, where the ν_j define equal increments

$$\Delta F(\nu_k) = F(\nu_k) - F(\nu_{k-1}) \tag{4.2b}$$

in $F(\nu)$, the unnormalized cumulative spectral distribution function. The sampled fequency ν is then calculated by using the truncation of a random number to find a value of k, followed by an interpolation between the appropriate values ν_k and ν_{k-1}. The tabulation of the cross section data should be available for the same ν_k values. It should be emphasized that the speed of the calculation is in no way affected by the size and complexity of the cross section data tables and that because of the effective scattering feature of the calculation the sampling from the spectrum is much more accurate than could be achieved with a limited number of source particles alone.

An alternative scheme is to represent the various contributions to absorption by simple analytic dependences such as $1/\nu^3$ for free-free absorption and bound-free absorption edges and Gaussian shapes for lines. It is then possible to express $\sigma_\nu b_\nu$ as

$$\sigma_\nu b_\nu = \sigma_p \sum_{n=1}^{N} p_n f_n(\nu), \tag{4.3a}$$

where the $f_n(\nu)$ are normalized emission distribution functions related to each contribution, e.g., edges, lines etc., and the p_n denote the weights of the individual contribution, or the $f_n(\nu)$ may refer to individual pieces of the complete emission spectrum. The p_n must, of course, satisfy

$$\sum_n p_n = 1. \tag{4.3b}$$

In order to sample from the distribution (4.3a) it is first necessary to sample from the discrete distribution p_n to determine n, and then to sample from the corresponding distribution $f_n(\nu)$, which is easily done.

If σ_ν has the form

$$\sigma_\nu = (1 - e^{-h\nu/kT})\, D/\nu^3, \tag{4.4}$$

then $\sigma_\nu b_\nu$ becomes

$$\sigma_\nu b_\nu = \sigma_p \left(\frac{h}{kT}\right) e^{-h\nu/kT}, \tag{4.5}$$

where use has been made of the expression

$$B_\nu = \frac{8\pi h\nu^3/c^3}{e^{h\nu/kT} - 1}. \tag{4.6}$$

One also obtains

$$\sigma_p = \frac{8\pi D}{c^3}\left(\frac{kT}{u_r}\right), \tag{4.7}$$

and, for constant b,

$$\beta\sigma_p = \frac{32\pi D}{c^3}\left(\frac{k}{b}\right). \tag{4.8}$$

The calculation of σ_p, $\beta\sigma_p$, and f is carried out and stored for each spatial zone at the beginning of each integration cycle.

B. *Apportionment of Source Particles*

Source particles are assigned to spatial zones and radiating surfaces in numbers which are roughly proportional to the amount of energy radiated in the particular location during the current integration cycle. At the beginning of the problem a fixed number of source particles N_S is injected during each cycle. If this number is wisely chosen, the attrition of particles by absorption and escape will insure that

$$N_C + N_S \leqslant N, \tag{4.9}$$

where N_C is the number of census particles waiting to be processed at the beginning of the time cycle, and N is the total number of particles for which storage space is available. Actually Eq. (4.9) allows a certain amount of leeway since the number of particles surviving the integration cycle and needing storage will be less than $N_C + N_S$. Whenever possible, N_S is chosen to be an input number

$$N_S = N_S^I, \tag{4.10}$$

but if condition (4.9) cannot be met, N_S is taken to be

$$N_S = N - N_C - N_Z - 1, \tag{4.11}$$

where N_Z is the number of space zones in the problem. Experience has shown that condition (4.11) insures stabilization of the census population without overly reducing the number of source particles.

If the surface of the slab $x = 0$ is kept at a fixed temperature T_0, the total energy radiated from that surface during an integration cycle of duration Δt is

$$E_S = \frac{ac}{4} T_0^4 \Delta t, \tag{4.12}$$

while the source energy radiated by cell $j - \frac{1}{2}$ is

$$E_{j-1/2} = f(T^n_{j-1/2})\, \sigma_p(T^n_{j-1/2})\, cu^n_{rj-1/2}\, \Delta x\, \Delta t + [1 - f(T^n_{j-1/2})]\, S^\gamma_{j-1/2}\, \Delta x\, \Delta t. \tag{4.13}$$

Depending on circumstances, accuracy may be improved by employing forward extrapolated temperatures in calculating f and σ_p. The total source energy radiated is

$$E_{\mathrm{TOT}} = E_{\mathrm{S}} + \sum_j E_{j-1/2}. \tag{4.14}$$

The number of surface source particles is taken to be

$$N_{\mathrm{SURF}} = \mathrm{int}\left(\frac{E_{\mathrm{S}} N_{\mathrm{S}}}{E_{\mathrm{TOT}}}\right) + 1, \tag{4.15a}$$

and the number of source particles in zone j is taken to be

$$N_{j-1/2} = \mathrm{int}\left(\frac{E_{j-1/2} N_{\mathrm{S}}}{E_{\mathrm{TOT}}}\right) + 1, \tag{4.15b}$$

where int signifies the integer part of the argument.

C. *Source-Particle Initial Data*

The energy of each surface source particle is given by

$$e_{\mathrm{SURF}} = (ac/4)\, T_0^4\, \Delta t / N_{\mathrm{SURF}}, \tag{4.16a}$$

while that of volume source particles is

$$e_{j-1/2} = E_{j-1/2} / N_{j-1/2}. \tag{4.16b}$$

The frequency of surface source particles is obtained by sampling from the normalized blackbody distribution

$$b(x) = \frac{15}{\pi^4} x^3/(e^x - 1), \tag{4.17a}$$

$$\nu = (kT/h)x. \tag{4.17b}$$

An efficient scheme for accomplishing this, based upon a series representation of the Planck function and developed by C. Barnett and E. Canfield (12), is detailed in Fig. 1. The efficiency of this scheme is 1.1 trials per selection. The frequency

$$\nu = (kT/h)\,|\ln r\,|, \tag{4.18}$$

where r signifies a random number distributed uniformly within the interval from 0 to 1.

The positions of volume source particles are uniformly distributed within the zone of origin, i.e., for zone $j - \frac{1}{2}$

$$x = x_{j-1} + r(x_j - x_{j-1}), \tag{4.19}$$

where x_j and x_{j-1} are coordinates of zone interfaces, while the direction cosine μ is uniformly distributed between -1 and 1:

$$\mu = 1 - 2r. \tag{4.20}$$

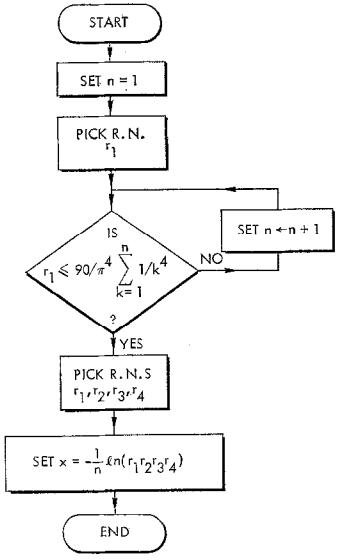

FIG. 1. Flow diagram for selection of frequencies from a Planck or blackbody spectrum.

The position of the surface source particles is of course $x = 0$, and the direction cosines are distributed according to

$$f(\mu) = 2\mu, \tag{4.21}$$

or

$$\mu = \max(r_1, r_2). \tag{4.22}$$

The emission time for source particles is uniformly distributed over the integration cycle, or

$$t = t^n + r(t^{n+1} - t^n). \tag{4.23}$$

D. *Geometry*

The geometry calculation consists of determining the distance traveled by a particle

$$d = \min(d_{\mathrm{B}}, d_{\mathrm{COL}}, d_{\mathrm{CEN}}) \tag{4.24}$$

where d_{B}, d_{COL}, d_{CEN} are respectively distances to a boundary crossing, a scattering collision, or to census. For a particle in zone $j - \frac{1}{2}$ these quantities are

$$d_{\mathrm{B}} = \begin{cases} (x_j - x)/\mu & \text{if } \mu > 0, \\ (x_{j-1} - x)/\mu & \text{if } \mu < 0, \end{cases} \tag{4.25a}$$

$$d_{\mathrm{COL}} = |\ln r|/(1 - f_{j-1/2})\,\sigma_\nu, \tag{4.25b}$$

$$d_{\mathrm{CEN}} = c(t^{n+1} - t). \tag{4.25c}$$

If either d_{B} or d_{CEN} are selected, particle data are advanced according to

$$x' = x + \mu d, \tag{4.26a}$$

$$t' = t + d/c, \tag{4.26b}$$

$$E' = Ee^{-f\sigma_\nu d}, \tag{4.26c}$$

$$\nu' = \nu, \tag{4.26d}$$

$$\mu' = \mu. \tag{4.26e}$$

Here E' and E refer to energy carried by the particle. The particle's energy loss

$$\Delta E = E(1 - e^{-f\sigma_\nu d}) \tag{4.27}$$

is added to the total radiation energy $\mathscr{E}_{j-1/2}$ already deposited in the zone. If E' is less than or equal to 1 % of the particle's energy at birth, the particle is eliminated, and its total energy is added to $\mathscr{E}_{j-1/2}$. If $d = d_{\mathrm{CEN}}$ the particle's data are stored for use in the next integration cycle. If $d = d_{\mathrm{B}}$, a new value of σ_ν is calculated, and the geometry routine is reentered.

Should d_{COL} be selected, x', t', and E' are advanced, energy is deposited as before, and ν' is selected by sampling from the volume source particle frequency distribution, e.g., Eq. (4.18). A new value of σ_ν is calculated and the direction cosine is chosen to satisfy Eq. (4.20). The geometry routine is then reentered.

E. *Energy Update and Energy Check*

The updated temperature is obtained by solving Eq. (4.1e) or

$$T^{n+1}_{j-1/2} = T^{n}_{j-1/2} + b^{-1}(T^{n+1/2}_{j-1/2})\{\mathscr{E}_{j-1/2}/\Delta x - f_{j-1/2}c\Delta t\sigma_{pj-1/2}u^{n}_{rj-1/2} + f_{j-1/2}S^{\gamma}_{j-1/2}\,\Delta t\} \tag{4.28}$$

In such calculations it is usual to calculate an "energy check" which is defined as

$$E_{\text{CHK}} = (E_{\text{inp}} - E_{\text{int}})/E_{\text{inp}}\,, \tag{4.29}$$

Where E_{inp} is the net energy input into the system and E_{int} is the total internal energy of the system consisting of both the radiation and material energy. Since the application of Eq. (4.28) enables us to carry out the energy bookkeeping

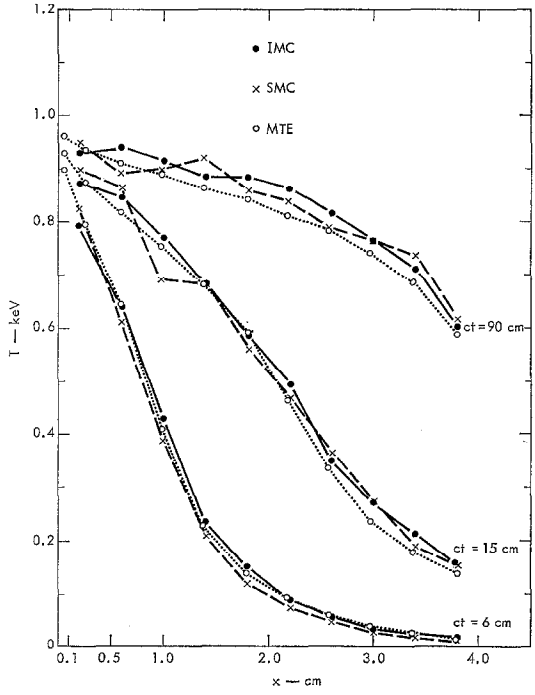

FIG. 2. Radiation penetration of a slab heated by 1 KeV source at $x = 0$. Comparison between implicit Monte Carlo (IMC), semiimplicit Monte Carlo (SMC), and multigroup telegrapher's equation solutions (MTE) for temperature distribution. Cross section has $1/\nu^3$ dependence given by Eq. (5.1); $\Delta x = .4$ cm, $\Delta t = 2 \times 10^{-3}$ sh for IMC.

exactly, in principle, the energy check should be limited only by the accuracy of the computer in carrying out arithmetic operations. In the case of the CDC 7600 this leads to values of the order of 10^{-12}. For larger values than this one should suspect programming errors.

One can also use the exact energy balance method in a purely explicit scheme,

in which case $f = 1$ in Eqs. (4.1) and (4.26). Unfortunately, this scheme is known to be unstable for

$$\alpha\beta c\Delta t\sigma_p \sim 1, \tag{4.30}$$

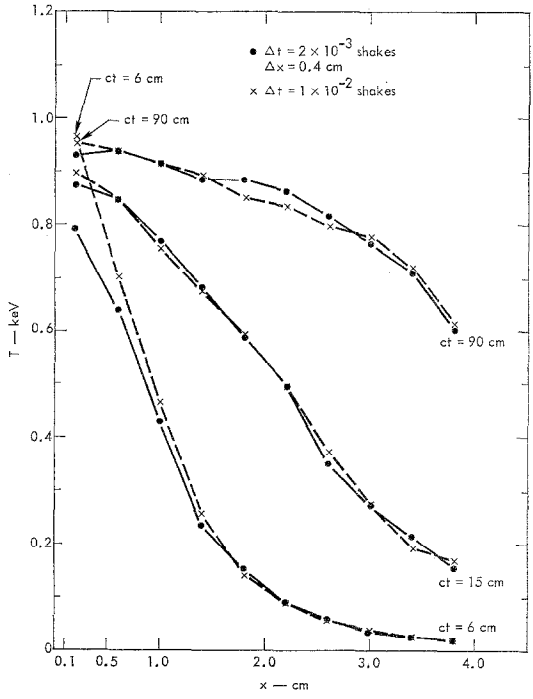

FIG. 3. Comparison between IMC temperature solutions for $\Delta x = .4$ cm, $\Delta t = 2 \times 10^{-3}$ sh, and $\Delta t = 1 \times 10^{-2}$ sh, cross section given by Eq. (5.1). The scattering fraction $1 - f$ in the two cases are .944 and .988, respectively.

i.e., when Δt is roughly equal to the relaxation time for the matter temperature to equilibrate with the radiation field. An explicit scheme which has improved stability is obtained by setting $f = 1$ and replacing $u(T^n_{j-1/2})$ with $u(T^{n+1}_{j-1/2})$ in Eq. (4.28) and solving the resulting nonlinear equation by an iterative method [1]. This method, sometimes referred to as "semi-implicit," does not conserve energy, and energy checks in typical problems may run as high as 20%. By employing effective scattering, one has the double advantage of both exact energy conservation and what appears to be unconditional stability.

V. Numerical Examples

A comparison of an implicit Monte Carlo (IMC), a semi-implicit Monte Carlo (SMC) (see above, Sec. IV-E), and a 27-group telegrapher's equation calculation [13] is shown in Fig. 2 for a slab 4 cm in thickness, heated by a 1 KeV blackbody source at $x = 0$, and having a macroscopic cross section given by

$$\sigma_\nu = \frac{27}{\nu^3}(1 - e^{-\nu/T})\ \text{cm}^{-1}, \tag{5.1}$$

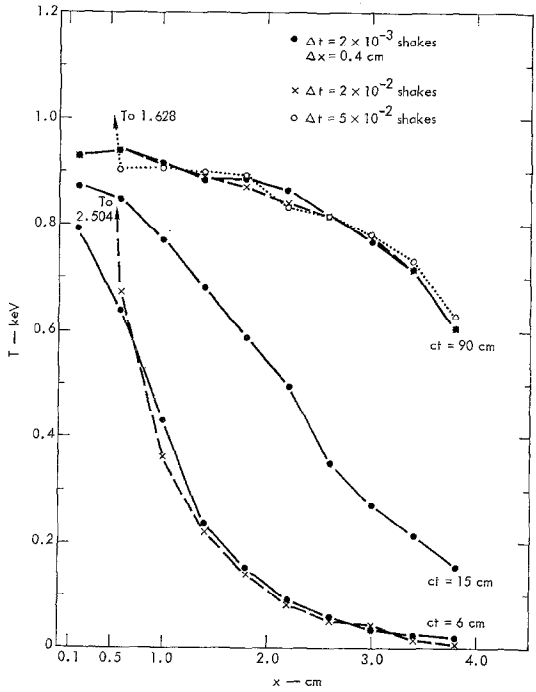

FIG. 4. Comparison between IMC temperatures for $\Delta x = .4$cm, $t = 2 \times 10^{-2}, \Delta t = 5 \times 10^{-2}$sh. Cross section given by Eq. (5.1). Scattering fractions are .944, .994, .998, respectively.

where ν, and T are measured in keV. This cross section, it will be noted, has a value of 1.0 cm^{-1} for $\nu = 3$ KeV, which is approximately the frequency for which a 1 keV blackbody spectrum peaks. The temperatures in all zones are set equal to .001 keV initially to keep σ_p finite. The value of b for this and all subsequent figures is taken to be .5917 a T_0^3. The resulting scattering fraction for the IMC calculation is constant with temperature and equal to 94.4% with $\alpha = 1$. At late

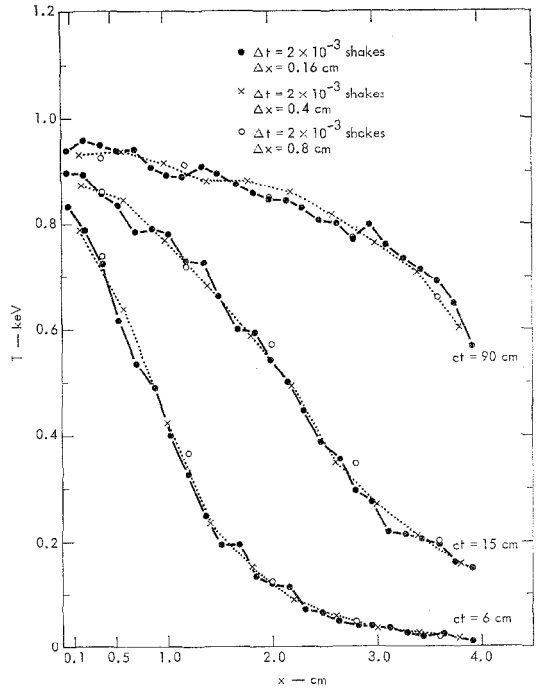

FIG. 5. Temperature distributions calculated by IMC for three different spatial zone sizes: $\Delta x = .16$ cm, $\Delta x = .4$ cm, and $\Delta x = .8$ cm and cross section given by Eq. 5.1.

times the SMC calculation has an energy discrepancy, $E_{CHK} \sim 20\%$. In addition, for $ct = 90$ cm, by which time equilibrium has been established, the SMC calculation has been averaged over 50 cycles to smooth fluctuations. No averaging of the IMC has been used. Both calculations employ the same spatial step size $\Delta x = .4$ cm. The IMC calculation utilizes a constant $\Delta t = 2 \times 10^{-3}$ sh (1 shake $= 10^{-8}$ sec.). Information is unavailable on the SMC integration cycle times for this particular calculation, but an SMC calculation with the same parameter values and yielding substantially the same results was carried out with an average $\Delta t \sim 1.7 \times 10^{-3}$ sh [14]. A purely explicit calculation would become unstable for $\Delta t \sim 10^{-4}$ sh. In all IMC calculations reported here, cross sections, f-values, and blackbody spectra have been calculated using temperature values available at the end of the previous integration cycle. Except as noted above, the IMC and SMC calculations appear to be in reasonable agreement.

Figures 3 and 4 illustrate the stability of the IMC solutions with increasing values of Δt. In Fig. 3 the $ct = 6$ cm curve for $\Delta t = 1.0 \times 10^{-2}$ sh is slightly high for the zone nearest the source, but by the time ct = 15 cm the solution has

corrected itself. In Fig. 4 the $ct = 6$ cm curve is inaccurate near the source for $\Delta t = 2 \times 10^{-2}$ sh, although the remainder of the curve does not look bad. By the time $ct = 90$ cm, the $\Delta t = 2 \times 10^{-2}$ sh solution is accurate. Note also that for $ct = 90$ cm the $\Delta t = 5 \times 10^{-2}$ sh solution is also accurate with the exception of the zone closest to the source. In the latter calculation the problem was completed in only 6 integration cycles! Undoubtedly results for large time cycles could be improved by employing forward extrapolated temperatures in the calculation of temperature-dependent parameters. Figures 3 and 4, however, lend considerable credence to the assumption that IMC is unconditionally stable and that cycle durations can be chosen solely on the basis of accuracy considerations.

Figure 5 shows the influence of zone size on the temperature distribution. It is seen that decreasing the zone size from .4 cm to .16 cm does not improve the accuracy of the solution but instead introduces a slight spatial fluctuation. Figure 6 shows the effect of decreasing the time cycle for a .16 cm zone problem. A time cycle of 2×10^{-4} sh enhances fluctuations slightly. Figure 7 is a comparison of a "fully" implicit calculation with $\alpha = 1$ and a "partially" implicit calculation with

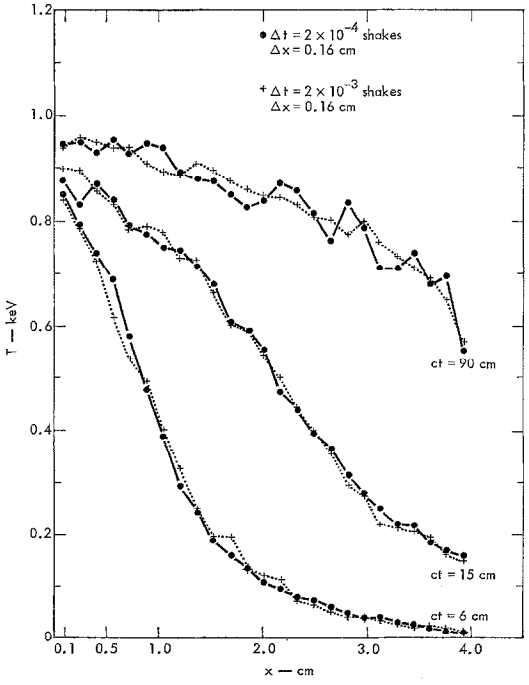

FIG. 6. Temperature distributions for 2 different values of Δt: $\Delta t = 2 \times 10^{-3}$ sh and $\Delta t = 2 \times 10^{-4}$ sh, cross section given by Eq. (5.1) and $\Delta x = .16$ cm.

$\alpha = \frac{1}{2}$, both for $\Delta t = 2 \times 10^{-4}$ sh and $\Delta x = .16$ cm. The scattering fractions are 63 % and 46 %, respectively. Fluctuations tend to be greater at later times for the $\alpha = \frac{1}{2}$ calculation. This effect should be only partially attributable to the fact that the $\alpha = 1$ case is run with a slightly larger mean population. One can conclude from Figs. 2–7 that by running with large time steps and, consequently, large scattering fractions the tendency is for statistical fluctuations to be reduced.

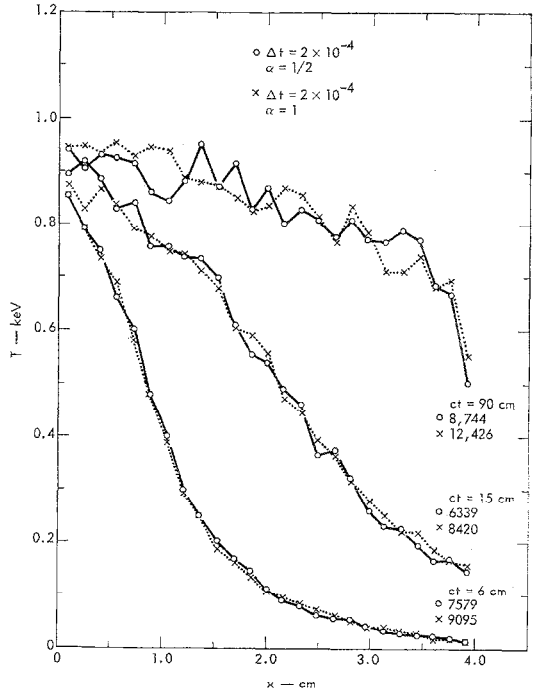

FIG. 7. Comparison of "fully" implicit, $\alpha = 1$, and "partially" implicit $\alpha = 1/2$ calculations of temperature for $\Delta t = 2 \times 10^{-4}$ sh. Scattering fractions are $1 - f = 63\,\%$ and 46 %, respectively. History numbers at different times are indicated.

Figure 8 shows the effect of including an additional $T^{-3/2}$ dependence of cross section on temperature, where

$$\sigma_\nu = \frac{27}{\nu^3 T^{3/2}} (1 - e^{-\nu/T}) \text{ cm}^{-1}. \tag{5.2}$$

The temperature in all zones is initially set equal to .01 KeV in order to keep the cross sections finite. Despite the fact that initially scattering fractions go as high as 99.94 % and cross section values exceed those of Eq. (5.1) by a factor of 10^3,

no calculational difficulties are encountered. Although in the case of Eq. (5.2) the break in the radiation front is more abrupt, it will be noted that, behind the front, temperatures exceed those for the case of Eq. (5.1).

Figures 9A and 9B show results of both temperature and radiation energy density calculated for the case of an absorption edge at $\nu = 3$ KeV. The cross section assumed is

$$\sigma_\nu = \begin{cases} \dfrac{24}{\nu^3}(1 - e^{-\nu/T}), & \nu < 3 \text{ KeV}, \\ \dfrac{54}{\nu^3}(1 - e^{-\nu/T}), & \nu \geqslant 3 \text{ KeV}. \end{cases} \tag{5.3}$$

The radiation energy density is calculated by averaging over particle tracklengths in each zone. As would be expected, the radiation penetrates more rapidly than the equilibrium radiation energy density variable u_r. The criss-crossing behavior of the radiation energy density and u_r curves for $ct = 90$ cm is due to fluctuations inherent in solutions at equilibrium.

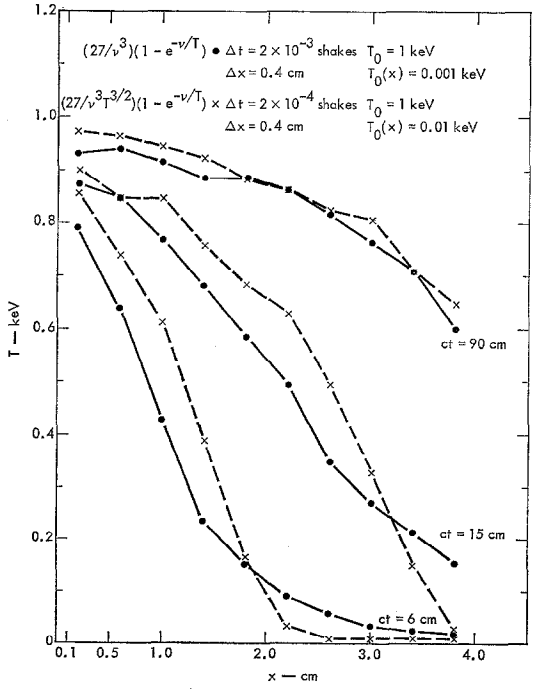

FIG. 8. Comparison of temperature distributions for cross section calculated by Eqs. (5.1) and (5.2). Equation (5.2) differs from (5.1) by factor $T^{-3/2}$.

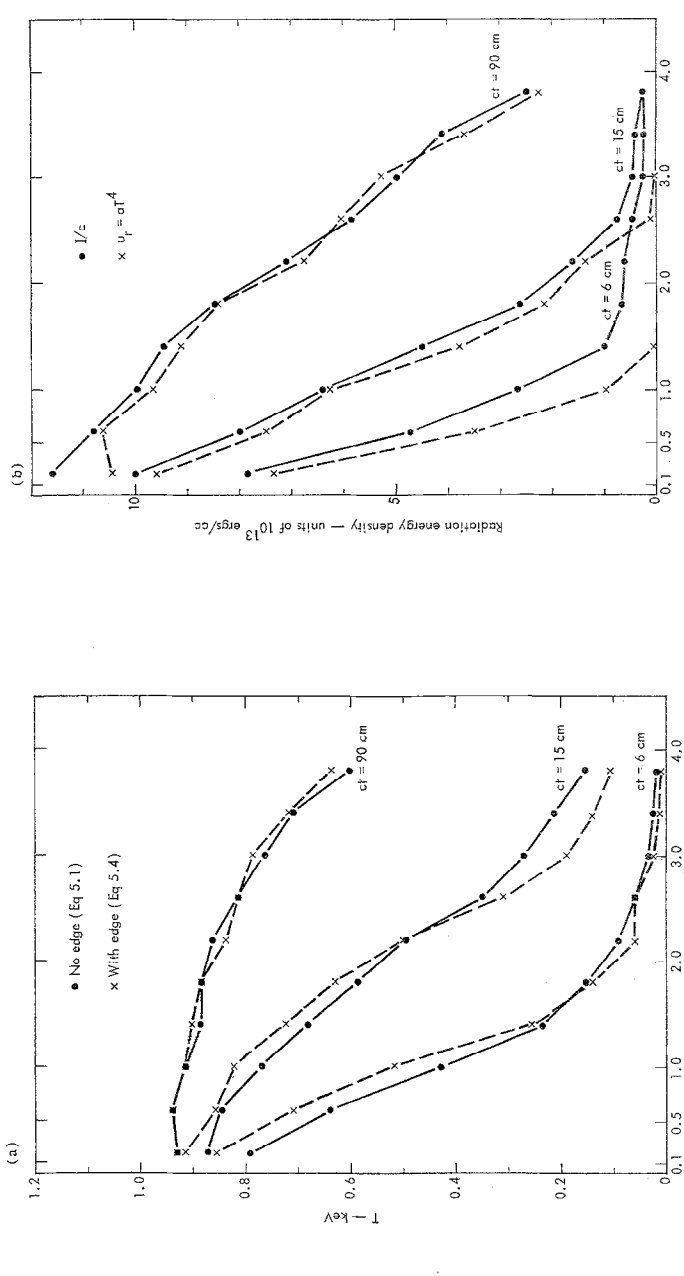

FIG. 9. Slab penetration for cross section having a single absorption edge. (a) Temperature compared with that for Eq. (5.1); (b) Comparison between equilibrium energy density $u_r = aT^4$ and actual radiation energy density I/c.

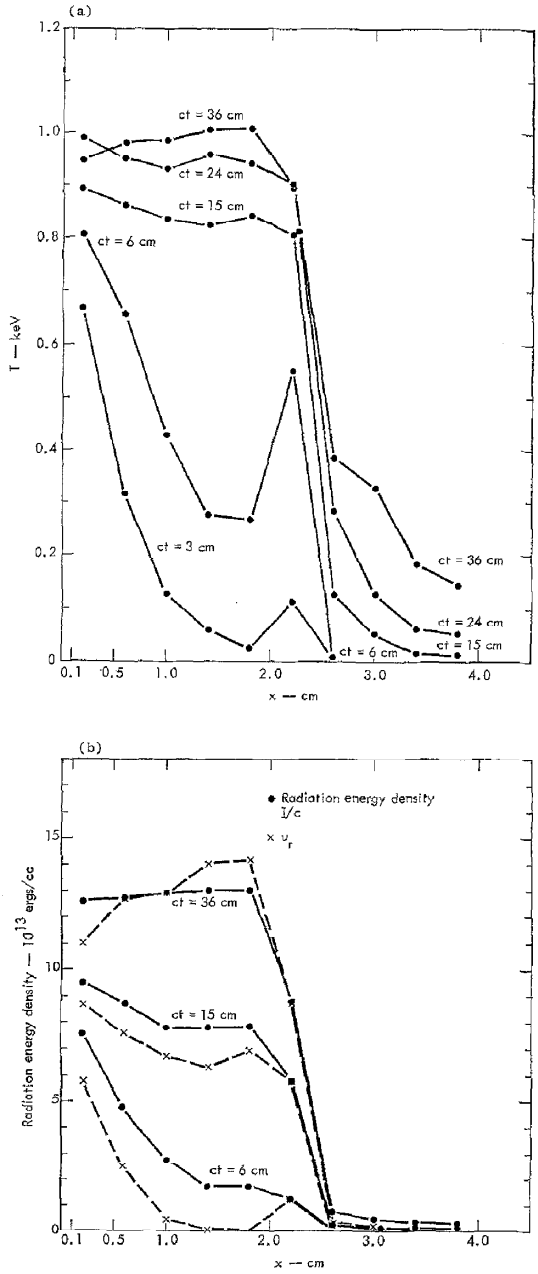

FIG. 10. Slab penetration $\Delta t = 2 \times 10^{-8}$ sh, $\Delta x = .4$ cm, single opaque zone extending from $x = 2.0$ to $x = 2.4$, $\sigma_\nu = (10{,}000/\nu^3)\, x(1 - e^{-\nu/T})$. Otherwise σ_ν given by Eq. (5.1). (a) Temperature profiles. (b) Comparison between equilibrium radiation energy density $u_r = aT^4$ and actual radiation energy density I/c.

The utility of the effective scattering method when optically thick media are encountered is illustrated in Fig. 10. The conditions for Fig. 10 are the same as for Fig. 1, except that in the zone extending from $x = 2.0$ to 2.4 cm the cross section is assumed to be given by

$$\sigma_\nu = \frac{10{,}000}{\nu^3}(1 - e^{-\nu/T})\ \text{cm}^{-1}. \tag{5.4}$$

In the opaque zone the Planck mean cross section σ_p varies from a maximum of $10^{12}\ \text{cm}^{-1}$ at the start of the problem to a minimum of $2 \times 10^3\ \text{cm}^{-1}$ by the end of the problem, compared with a minimum value of $\sim 5\ \text{cm}^{-1}$ in the transparent zones [15]. The examples of Figs. 8 and 10 indicate that difficulties or complications with the method are not anticipated when cross sections become large, although if large regions of the problem contain highly opaque materials, one may be forced to pay a high price in computing time (see Table I).

TABLE I

Comparison of Characteristics for Various Implicit Monte Carlo Calculations

Figure	σ_ν (Eq.)	Δx(cm)	Δt(sh)	Cycles (No.)	N_S	Particle No. final cycle	Running time (min) CDC 7600	Scattering fraction $(1 - f)$
Not shown	(5.1)	.4	2×10^{-4}	1500	500	12,134	13.0	.628
2, 3, 4, 5	(5.1)	.4	2×10^{-3}	150	1000	11,175	5.90	.944
5, 6	(5.1)	.16	2×10^{-3}	150	1000	11,283	6.5	.944
3	(5.1)	.4	1×10^{-2}	30	3000	12,303	5.85	.988
4	(5.1)	.4	2×10^{-2}	15	4000	6,186	5.10	.994
4	(5.1)	.4	5×10^{-2}	6	5000	8,132	6.5	.998
4	(5.2)	.4	2×10^{-4}	1500	200	4,996	16.24	.9994[a]
9	(5.3)	.4	2×10^{-3}	150	500	5,939	2.84	.938
10, 11b	(5.4)	.4	2×10^{-3}	60	500	6,166	44.3	.9998[b]

[a] First cycle.
Fifth zone.

Calculations of zone spectra are displayed in Figs. 11 and compared with blackbody spectra at the appropriate zone temperatures. Figure 11a is for the calculation of Fig. 2 and applies for $ct = 90$ cm and for the zone centered at $x = 1.4$ cm. Figure 11b is for $ct = 12$ cm and for the opaque zone in the problem

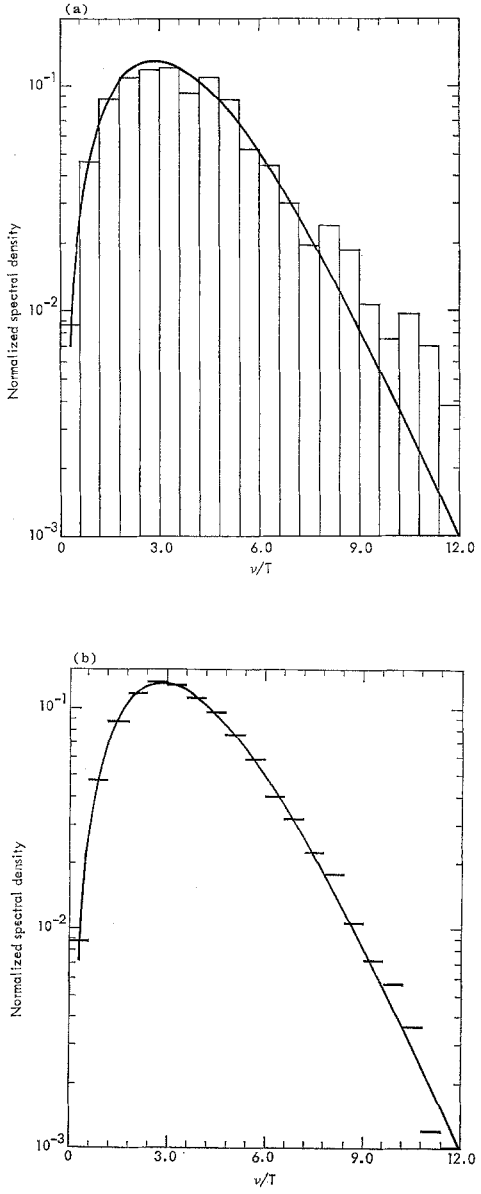

FIG. 11. Zone spectra over single integration cycle compared with blackbody spectrum at zone temperature. (a) Zone centered at $x = 1.4$ cm, $ct = 90$ cm, temperature distribution shown in Fig. 2, (b) Opaque zone centered at $x = 2.6$ cm, $ct = 12$ cm, temperature distribution given in Fig. 10.

of Fig. 10. These spectra were calculated by path length [illegible]

in particle populations for the different cases make accurate comparisons in running time difficult, it may be concluded that, given like numbers of histories, the implicit Monte Carlo method leads to improvements in running time as integration cycles are lengthened, at least up to a point. As the scattering fraction $1 - f$ approaches 1.0, the problem running time is governed primarily by the length of time necessary to perform a particle scattering and by the frequency of particle scatterings. If f is exceedingly small, many scattering events may be required before a particle comes to extinction. Therefore, exceedingly large values of Δt may not guarantee the shortest problem running times. In fact, experience indicates that when the scattering fraction exceeds 99 %, increasing the time cycle may lead to diminished returns. One may therefore elect to control the time step so that f is never below 1 %. It may be practical, on the other hand, to arbitrarily set a floor of 1 % beneath f regardless of time step size, since the derivation of Eqs. (4.1) only limits the maximum value of f. Clearly, further experimentation is required to determine the most efficient method of operating with implicit Monte Carlo.

One should, at the very least, expect substantial improvements in running times over those required by a completely explicit scheme in which the integration cycle is controlled by stability considerations. Here an important distinction between the implicit and explicit schemes needs to be pointed out. In the case of an explicit calculation, essentially the same amount of work must be done in all zones with the value of Δt governed by the zone where instability is most likely to occur, usually the most opaque zone of the problem. In the case of the implicit method the most calculation is, in general, required for the most opaque zones and the least for the transparent zones. This feature alone should lead to significant savings in calculation time for the implicit over the explicit scheme. In addition it should be possible to operate the implicit scheme with a smaller number of particles for a given level of statistical accuracy.

It should be mentioned, finally, that for the second and last problems of Table I a reduction by one-third from the running times listed could be achieved by calculating all exponentials and logarithms through a table lookup procedure.

Conclusion

The conclusion to be drawn from these numerical studies is that the implicit Monte Carlo treatment of nonlinear radiation transport problems leads to a significant improvement in accuracy, stability, overall flexibility, and computa-

tional efficiency, over the explicit methods which have been previously employed. While the implicit Monte Carlo method does not offer a complete panacea for all running time problems, it does make feasible the solution of a wide range of problems within the framework of a single calculational method, which smoothly spans conditions ranging from those where pure transport theory applies to those which normally require the application of diffusion theory.

ACKNOWLEDGMENT

The authors wish to express indebtedness to Nelson Byrne, Eugene Canfield, and Alan Winslow for valuable discussion.

REFERENCES

1. J. A. FLECK, JR., *in* "Computational Methods in the Physical Sciences" (B. Alder and S. Fernbach, Eds.), Vol. 1, p. 43, McGraw-Hill, New York, 1963.
2. P. M. CAMPBELL AND R. G. NELSON, "Numerical Methods for Nonlinear Radiation Transport Calculations," Report UCRL-7838, Lawrence Radiation Laboratory, Livermore, Calif., 1964.
3. The VERA Code, A One-Dimensional Radiative Hydrodynamic Program, Systems, Science, and Software Report, 3 SR-29(1968).
4. H. L. WILSON, to be published.
5. For analysis of the stability of multifrequency finite difference equations see J. T. PALMER AND D. R. SMITH, *J. Comp. Phys.* **6** (1970), 356.
6. The use of the term "photon" is avoided in this context, since the energy carried by such particles is in general not a linear function of frequency.
7. A treatment of time-independent radiative transfer using an effective scattering model is discussed by J. C. STEWART, I. KÛŜCER, N. J. MCCORMICK, *Ann. Phys.* **40** (1966), 321, using somewhat restrictive assumptions on the variation of cross section with frequency.
8. Normally, one assumes that if a numerical solution of a nonlinear transport problem is to be accurate in the diffusion regime, source terms should be approximated at least as linear functions of position across a spatial zone. We are claiming considerably more accuracy than this is possible in our treatment of source terms.
9. V. KOURGANOFF, "Basic Methods in Transfer Problems," Oxford, 1952.
10. An alternate way of advancing temperature, which guarantees energy conservation, is to upgrade u_m using Eq. (1.18). Temperature can then be calculated from u_m by means of a table.
11. It should be emphasized that even though T is regarded as a step function over zones, we are not making the same assumption regarding radiation sources, which are represented in part by effective scattering terms. See Ref. [8].
12. C. BARNETT AND E. CANFIELD, unpublished Lawrence Radiation Laboratory internal report.
13. The SMC and multi-group telegrapher's equation calculations were carried out by R. G. Nelson and are contained in unpublished Lawrence Radiation Laboratory internal reports.
14. W. E. LOEWE, unpublished Lawrence Radiation Laboratory internal report.
15. Actually, an accurate solution to this problem would require more than one zone in the opaque region. Our purpose here is to show that the IMC method can be applied without difficulty to an opaque problem with large zones relative to average mean free paths.